10th Pacific Symposium on Flow Visualization and Image Processing
Naples, Italy, 15-18 June, 2015

PIV measurements in the wake of two circular cylinders in tandem configuration with ground effect

Marco Raiola[1,*], Andrea Ianiro[1], Stefano Discetti[1]

[1]Aerospace Engineering Group, University Carlos III of Madrid, Leganés, Spain
*corresponding author: mraiola@ing.uc3m.es

Abstract PIV measurements have been performed in the near wake of two identical circular cylinders arranged in tandem configuration in the stream-wise direction and with additional interference of ground. The Reynolds number based on the cylinder diameter is 4900. Test have been performed for pitch-to-diameter ratios equal to 1.5, 3 and 6, corresponding respectively to the flow regimes of single bluff body, shear layer reattachment and vortex shedding of twin cylinders in absence of ground effect.
A splitter plate is introduced in the wind tunnel to remove the effect of the boundary layers developing on the tunnel walls. The gap between the cylinders and the splitter plate (modeling the ground) is set equal to 3, 1 and 0.3 diameters.
For the highest gap-to-diameter ratio cylinders shed vortices symmetrically in the wake and the measured vortical structures are consistent with tandem cylinders literature developed with no ground interference.
For a gap-to-diameter ratio equal 1, the ground strongly influences the wake, introducing asymmetry in the typical Von Karman shedding behavior. The wake is rotated far from the plate. The ground boundary layer is thickened past the second cylinder. At gap ratio 0.3 the typical Von Karman shedding structures are replaced by a jet-like structure ejected from the gap between the cylinder and the wall; the jet strongly changes the features of the shedding wake on the side opposite to that of the wall. Large recirculation structures are found behind the second cylinder.

Keywords: Tandem Cylinders, Ground Effect, Particle Image Velocimetry, Proper Orthogonal Decomposition

1 Introduction

The flow around arrays of cylinders immersed in a cross-flow is a typical engineering problem that can be found in many applications. Cylinder-like structures are typical elements, for example, of heat exchangers, cooling systems for nuclear power plants, offshore structures, buildings, chimneys, powerlines, struts, grids, screens, and cables. Often these structures work in close proximity, thus introducing strong interaction effects between their respective wakes, thus affecting both amplitude and frequency of the periodic flow oscillations. Similarly, ground-structure interaction can effectively modify the behavior of the flow surrounding these objects.
The periodic flow behavior generated by a cylinder or by a bluff-body in general, immersed in a cross flow has been widely studied. The formation of periodic shedding of counter rotating vortices, known as Von Karman vortices, gives rise to fluctuating forces and noise. The turbulent shedding occurs at a Strouhal number based on the cylinder diameter equal to about 0.2 in a range of Reynolds number 1300<Re<5000 (Fey et al. [6]).
The flow around two cylinders in tandem configuration has been widely studied by Igarashi [8] and Zdravkovich [20]. A complete review of the subject is given by Sumner [12]. Depending on the Reynolds number Re and on the ratio between the center-to-center longitudinal pitch and the cylinder diameter (L/D, abbreviated hereafter as the gap ratio) three main flow behaviors can be identified. At small pitch ratios (approximately $1 < L/D < 1.2\text{–}1.8$ according to Zdravkovich [20] or $1 < L/D < 2$ according to Zhou and Yiu [21], depending on the Re range) the Karman vortex shedding for the upstream cylinder is completely suppressed and the two cylinders act as a single bluff-body. This flow regime has been often defined as *“extended-body”* or *“single bluff-body regime”* (Fig.1a). At intermediate pitch ratios (approximately $1.2\text{–}1.8 < L/D < 3.4\text{–}3.8$ according to Zdravkovich [20] or $2 < L/D < 5$ according to Zhou and Yiu [21], depending on the range of Re) a complex flow behavior appears in the gap between the cylinders. Even if in this regime the flow can show different behaviors, it can be mostly characterized by the reattachment of the separated free shear layers from the upstream cylinder on the surface of the downstream cylinder. This

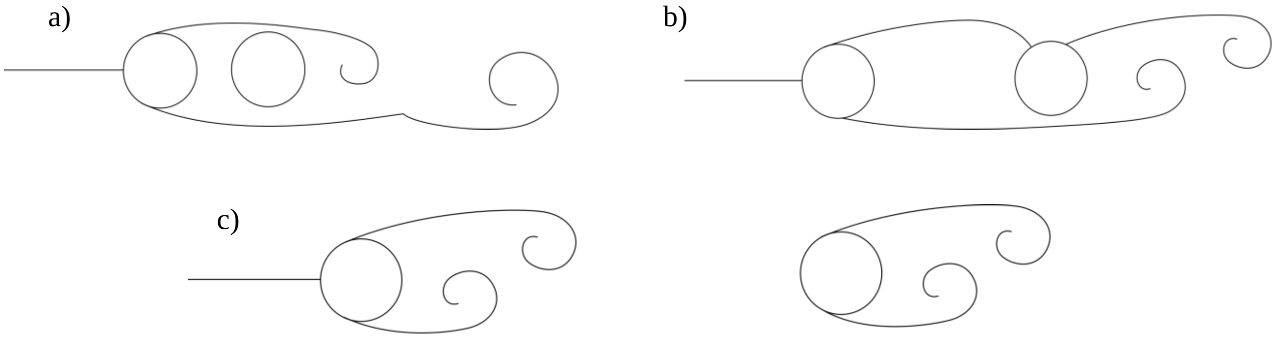

Fig. 1 Flow behaviors for cylinders in tandem configurations: a) *bluff-body regime*, b) *reattachment regime*, c) *co-shedding regime*.

regime is referred as *"reattachment regime"*(Fig.1b). At larger pitch ratios (approximately $L/D < 3.4\text{–}\ 3.8$ according to Zdravkovich [20] or $L/D < 5$ according to Zhou and Yiu [21], depending on the range of *Re*) both the cylinders develop a wake with the typical features of a Karman street. This regime is referred as *"co-shedding regime"* (Fig.1c). In the "*co-shedding regime"*, both the cylinders shed vortices at the same frequency, with the upstream cylinder shedding triggering the downstream one (Alam and Zhou [1]). The vortices shed from the downstream cylinder are larger in size but weaker in intensity than in the previous regimes (Zhou and Yiu [21]).

Xu and Zhou [19] shown that the Strouhal number related to vortex shedding is strongly affected by cylinder pitch ratio. For small pitch ratios the Strouhal number *St* is higher than 0.2 (shedding occurs at higher frequency than for an isolated cylinders). For higher pitch ratios, the Strouhal number decreases, reaching values lower than 0.2 in the *"reattachment regime"*. A discontinuous jump occurs when the flow behavior passes from *"reattachment"* to *"co-shedding regime"*. For higher pitch ratios the Strouhal number slowly approaches 0.2.

The effect of the ground proximity has been investigated for both circular (e.g., Lei et al. [9]; Price et al. [12]; Wang et al. [15]) and square (e.g., Martinuzzi et al. [11]; Wang and Tan [17]; Mahir [10]; Shi et al. [13]) single cylinders. Ground affects the pressure distributions, as well as the flow-induced vibration modes. The flow behavior is controlled by the ratio between the cylinder-to-wall gap height (measured from the cylinder surface closer to the wall, as in Fig.2)and the cylinder diameter (*G/D*, abbreviated hereafter as the gap ratio). For a critical gap ratio of about 0.3-0.5 the von Karman vortex shedding is suppressed as the wall poses an irrotational constraint on the cylinder wake (Zovatto & Pedrizzetti [22]). Little attention has been paid to the effect of the wall proximity on the case of two cylinders in tandem configuration. Bhattacharyya and Dhinakaran [5] investigated with numerical simulations a 2D flow around two near-wall tandem square cylinders (*G/D = 0.5*, *L/D = 1.5–6*, *Re=100-200*) with a shear velocity profile imposed upstream of them, and found that the cylinders wake resulted in a non-symmetric flow behavior: both non-uniformity of the flow and wall-induced vorticity weakens the vorticity of the lower separated shear layer with respect to the upper one. Harichandan and Roy [7] simulated numerically the flow around two near-wall tandem circular cylinders (*G/D = 0.5-1*, *L/D = 2-5*, *Re=100-200*). Their study revealed that for *L/D=5* the shedding frequencies of both upstream and downstream cylinders are equal. Moreover tandem cylinder wake is found to be less effective than the wake of single cylinder in destabilizing the downstream wall boundary layer and promoting separation. Wang et al. [16] measured with PIV the flow field around two square cylinders at *Re=6300* spanning a wide parametric space in both pitch ratio (*L/D=1.5, 2, 3, 4, 5, 6, 7*) and gap ratio (*G/D=0.25, 0.5, 0.75, 1, 1.5, 2*). Similarly to the case of the single cylinder for gap ratios below 0.5 the shedding is found to be suppressed. The interaction with the wall boundary layer is found to be relevant up to *G/D=1*.

A similar parametric study on near-wall circular cylinders in tandem configuration is not present in literature. In the present study the near-wake generated downstream of two circular cylinders in tandem configuration is investigated by means of PIV measurements. In Sec. 2 the experimental setup and the test conditions are described. The data collected from each experiment are used to calculate first and second order statistics; the results are presented in Sec. 3.

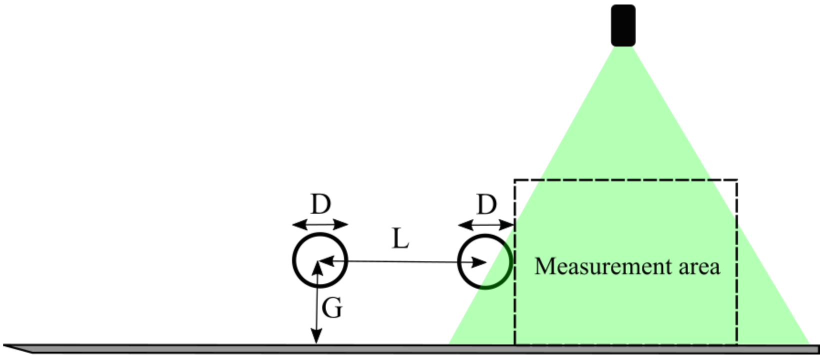

Fig. 2 A sketch of the experimental setup.

2 Experimental setup

The experimental study has been carried out in the recirculating wind tunnel of the Aerospace Engineering Group at University Carlos III of Madrid. This wind tunnel has a test section of 0.4 m x 0.4 m x 1.5 m. The ceiling and the lateral walls of the tunnel are made in methacrylate in order to achieve optical access for PIV measurements. Freestream turbulence intensity is estimated to be lower than 1%. The tunnel is equipped with a plane splitter plate with a sharp leading edge in order to minimize the boundary layer growth at the wall.

Two PVC cylinders, with diameter 32 mm and length 400 mm, are placed at half the height of the wind tunnel test section for the experiments. In Fig. 2 a sketch of the experimental setup is shown. The longitudinal position of the downstream cylinder is kept fixed in respect to the plate leading edge for all the experiments. The longitudinal position of the upstream cylinder and the vertical position of the plate in respect to the downstream cylinder are changed to vary the pitch ratio (*L/D*) and the gap ratio (*G/D*) respectively. Experiments are carried out for *L/D=1.5, 3* and *6* and *G/D=0.3, 1* and *3*. The wind tunnel velocity is kept fixed in order to achieve a Reynolds number based on the cylinder diameter of about 4900.

Velocity field measurements are performed with digital Particle Image Velocimetry in the near wake of the downstream cylinder. The flow is seeded with Di-Ethyl-Hexyl-Sebacate droplets with diameter of approximately 1 µm. The light source is a Big Sky Laser CFR400 ND:Yag (230 mJ/pulse). The acquisition is performed with a TSI PowerView™ Plus 2MP Camera (1600 × 1200 pixels resolution, 7.4 µm × 7.4 µm sensor size). An ensemble of 2000 image couples is acquired for each experiment.

The SPIV software, developed at University of Naples Federico II, is used to cross-correlate particle images and to calculate the velocity fields (Astarita & Cardone [4], Astarita [2],[3]). The interrogation strategy is an iterative multi-step image deformation algorithm, with final interrogation windows of 16x16 pixels, 50% overlap. Vector validation is carried out with a universal median test (Westerweel and Scarano [18]) on a 3x3 vectors kernel and threshold equal to 2 is used to identify invalid vectors. Discarded vectors are replaced with a distance-weighted average of neighbor valid vectors.

3 Results

The effects of a change in both the pitch ratio (*L/D*) and the gap ratio (*G/D*) on the flow behavior of the near wake of two circular cylinders in tandem configuration are shown in this section. The velocity fields measured from PIV are used to calculate the maps of the first and second order statistics of the flow field.

In Fig. 3 the maps of the streamwise component of the mean velocity are shown for all the cases considered in this study. In the first column the effect of a change in the pitch ratio are shown for the farthest distance from the ground (*G/D=3*) for which the effect of the ground can be neglected. For *L/D=1.5* the wake is relatively thin at few diameters from the downstream cylinders (about *1.4 D* at *x/D=2*). This behavior is consistent with the *"bluff-body regime"*, with the wake rolling up close to the downstream cylinder to form the von Karman vortices. The wake then increases in width, nearly doubling its width within few diameters downstream the cylinders (width is about *2.4 D* at *x/D=4*). For *L/D=3* the wake appears to be elongated in the streamwise direction if compared to the previous case. The wake width close to the downstream cylinder is larger (about *1.8 D* at *x/D=2*), while the rate of spreading of the wake appears slower (about *2.2 D* at *x/D=4*). This results still in a quite thin wake, which, however, presents a more severe defect of mass flow, indicative of a higher drag than the *"bluff-body"* case. This behavior seems consistent with a *"reattachment regime"*. For *L/D=6* the wake is wider than both the *"bluff-body"* case and *"reattachment"* case. The wake is few diameters thick downstream to the cylinders (nearly *3 D* at *x/D=2*). This indicates a severe mass flow defect produced by the upstream cylinder wake, so being consistent with a *"co-shedding regime"*. The wake appears quite long, producing a high defect of mass flow, and so on, a quite consistent drag.

The first row shows the effect of the gap ratio in the case *L/D=1.5*(*"bluff-body regime"* for the highest gap ratio *G/D=3*). For *G/D=1* the wake is slightly rotated far from the plate due to ground interaction. The mass flow defect presents a smoother and shorter peak at the same height of the cylinders than in the previous case. A stronger mass defect can be detected in the lower part of the wake, which tends to merge with the enlarged boundary layer of the plate after few diameters from the downstream cylinder. For *G/D=0.3* the effect of ground is stronger: the cylinder wake and plate boundary layer are completely merged producing a quite strong and diffused mass defect downstream the cylinders. On the upper side the wake stops growing after nearly 3 diameters from the downstream cylinder, likely due to the attachment of the wake to the plate.

The second row shows the effect of the gap ratio for the case *L/D=3* (*"reattachment regime"* for *G/D=3*). Similarly to the case *L/D=1.5*, for *L/D=3*and *G/D=1* the mass defect is increased in the lower part of the wake, close to the plate and is less intense at the same height of the cylinders. The gap produces a stronger flow with respect to the case *L/D=1.5, G/D=1*, so that boundary layer and wake merge at a larger streamwise distance from the downstream cylinder. For *L/D=3,G/D=0.3*, no separation between cylinder wake and boundary layer is present. The mass defect is higher than both the other cases, resulting in a more elongated wake.

The last row shows the effect of the gap ratio on the case *L/D=6*. For both *L/D=6, G/D=1*and *L/D=6, G/D=0.3* the wake of the cylinders and the boundary layer of the plate are nearly undistinguished. The defect of mass behind the cylinders appears to decrease for smaller *G/D* while the defect of mass produced in the gap seems to increase.

Fig.4 and Fig.5 present the maps of the normal streamwise component and of the in-plane shear component of the Reynolds stress tensor respectively. For the case *L/D=1.5, G/D=3* (*"bluff-body regime"*)both streamwise normal stress and in-plane shear stress shows strong symmetrical peaks at few diameters downstream of the cylinders. For *L/D=3* and *G/D=3* (*"reattachment regime"*) the stresses become weaker in intensity and interest a more elongated region. This is consistent with the picture of an elongated wake depicted before. For *L/D=6 G/D=3* (*"co-shedding regime"*) quite strong streamwise normal stresses interests a large portion of the wake. This can be addressed to the pulsating flow shed in the wake of the upstream cylinder and investing the downstream one. The Karman street shed by the downstream cylinder is convected by this pulsating flow, thus determining a more intense spatial spreading of the turbulent kinetic energy. The shear stresses instead appear weaker than the two previous cases.

With respect to the case *L/D=1.5, G/D=3*, both the cases *L/D=1.5, G/D=1* and *L/D=1.5, G/D=0.3* present a strong dissymmetry in the normal streamwise stresses, showing stronger streamwise oscillations closer to the plate. For the latter case, a strong peak is present close to the gap. More than to turbulence, this strong intensity of the fluctuating field can be addressed to a periodical mean flow, suggesting the presence of a pulsating-jet-like flow, whose periodicity is led by the shedding wake on the opposite side of the cylinder. A similar dissymmetry is present also in the shear stresses: for both the cases a lower positive shear stress is present closer to the ground.

At *L/D=3* the ground induced dissymmetry is less evident: the normal stress is a slightly stronger close to the plate in both the cases *L/D=3, G/D=1* and *L/D=3, G/D=0.3*. With decreasing gap ratio the shear stress appears weaker; moreover the lower part of the wake presents a weaker shear stress than its upper counterpart.

At *L/D=6* a similar effect of gap ratio is found on the shear stresses. The normal stress close to the plate, instead, appears to be weakened in the case *L/D=6 G/D=0.3*.

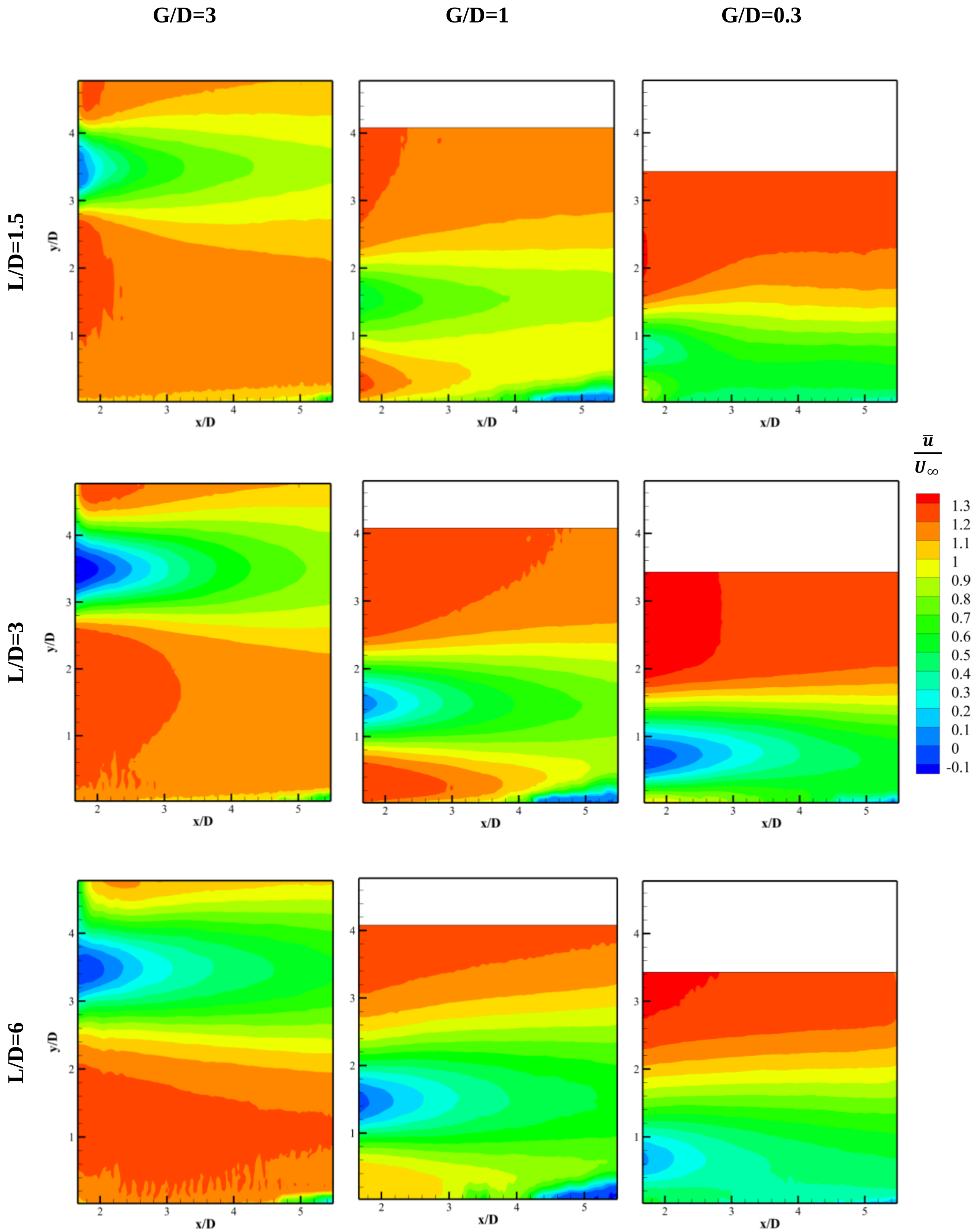

Fig. 3Contour maps of the average streamwise velocity component for all the pitch ratios (L/D) and gap ratios (G/D) object of the study. Re=4900. x distance is measured from the downstream cylinder center; y distance is measured from the splitter plate.

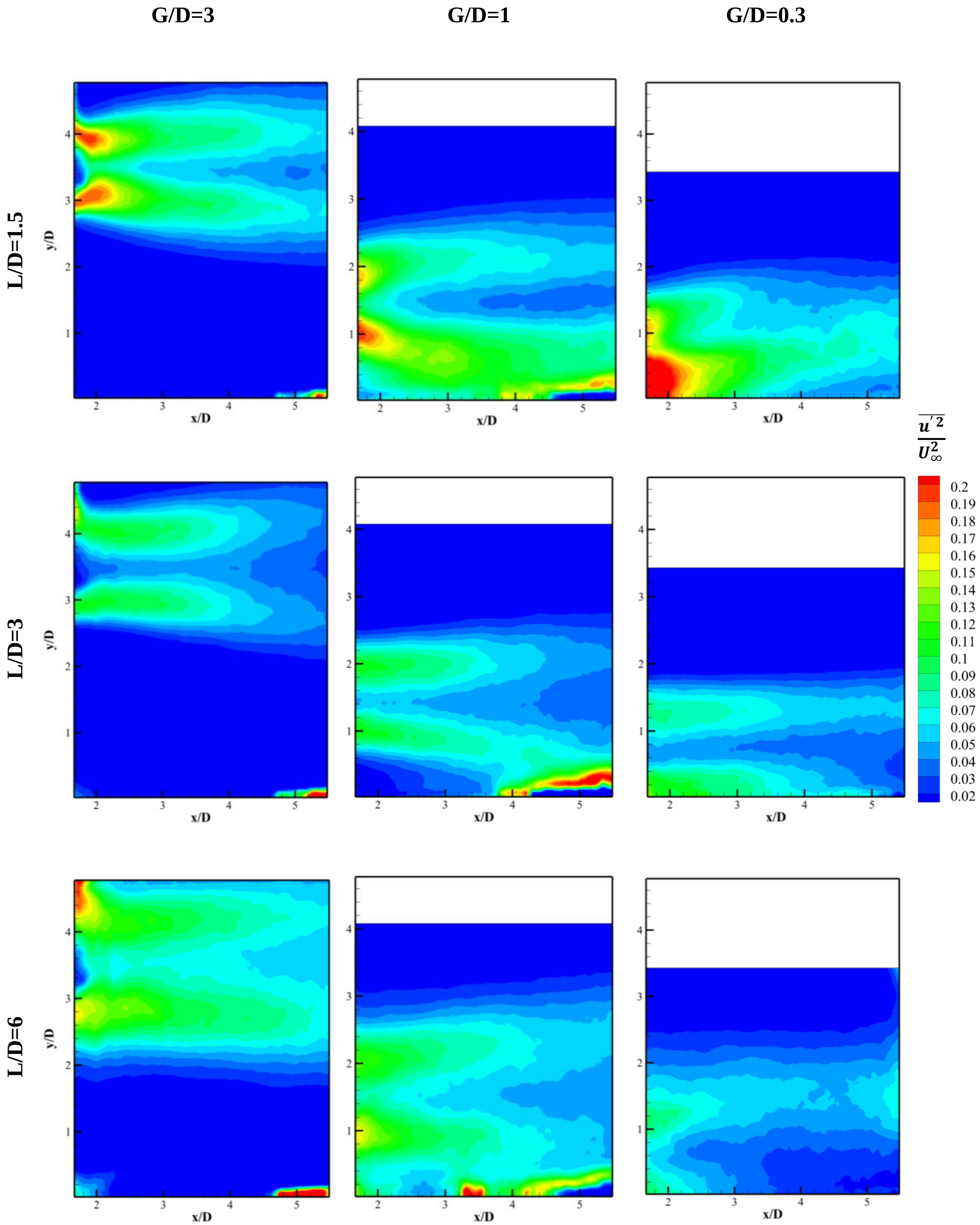

Fig. 4 Contour maps of the normal streamwise component of the Reynolds stress tensor for all the pitch ratios (L/D) and gap ratios (G/D) object of the study. Re=4900. x distance is measured from the downstream cylinder center; y distance is measured from the splitter plate.

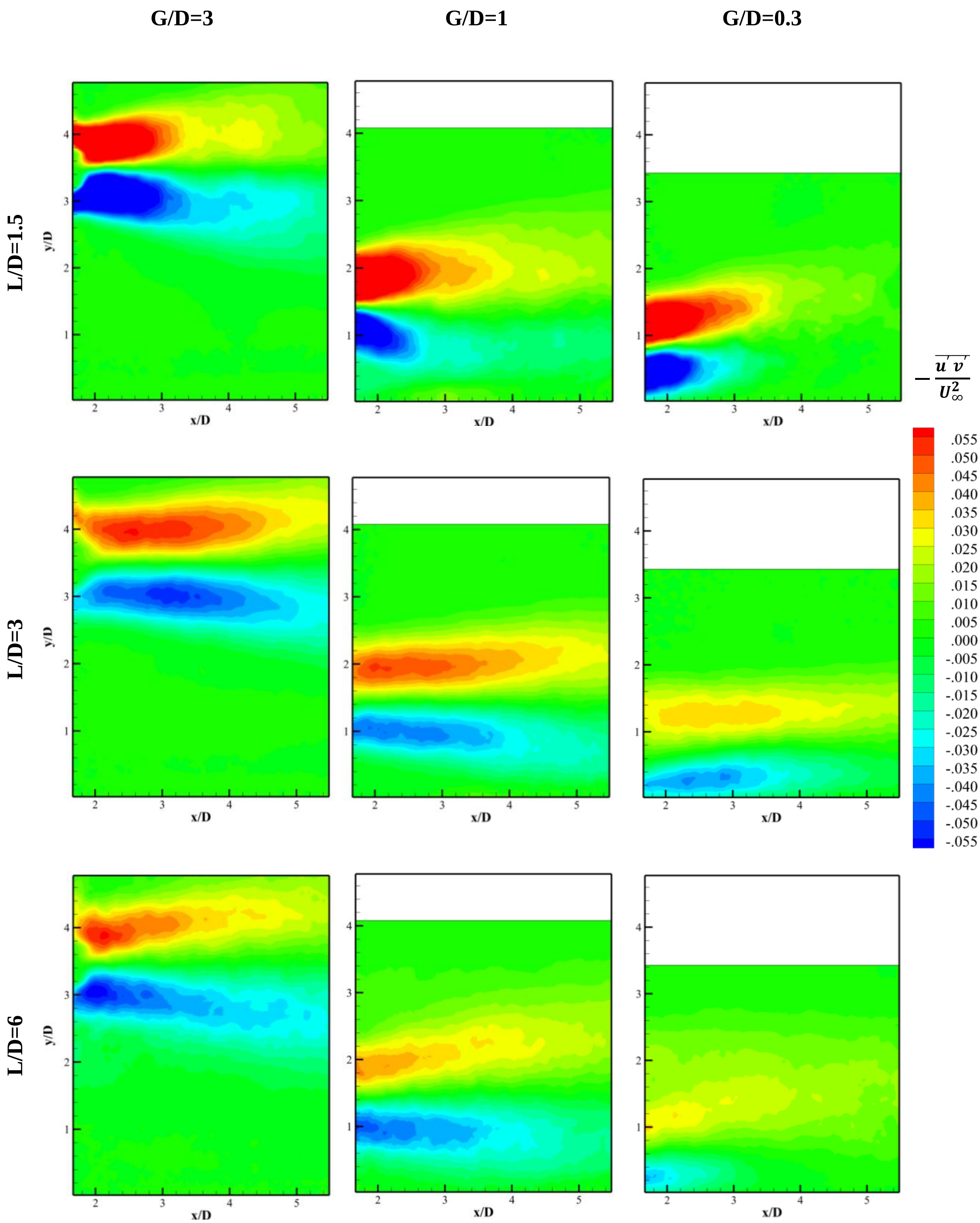

Fig. 5 Contour maps of the in-plane shear component of the Reynolds stress tensor for all the pitch ratios (L/D) and gap ratios (G/D) object of the study. Re=4900. x distance is measured from the downstream cylinder center; y distance is measured from the splitter plate.

4 Conclusion

A study on near-wall circular cylinders in tandem arragements has been performed. A parametric investigation on the effect of the distance between the cylinders and of the gap from the wall has been carried out. Measurements in the near wake of the downstream cylinder have been performed by means of PIV. The measured velocity fields are used to calculate first and second order statics of the flow fields.
The results highlight different near wake behaviors with varying cylinders pitch ratio for the highest cylinders-plate gap ratio. For small pitch ratios the wake is rather compact with well-defined Reynolds stress peaks. As the pitch ratio increases, the wake tends to elongate and mass flow defect is increased. The Reynolds stresses spread over a wider area as an effect of the pulsation of the incoming flow on the downstream cylinder.This phenomenology is similar to that of tandem cylinders with no ground effect, showing that at a gap of 3 diameters the presence of the plate has a negligible effect. For smaller gap ratios the effect of the ground produces a dissymetry in the wake, both due to the interaction with the plate boundary and to the formation of pulsating-jet-like features in the cylinder-plate gap. For the smallest pitch ratio and gap ratio this pulsating-jet-like feature produces a suction effect, leading to a significant deflection of the wake region towards the wall.
No information on shedding suppression at small gap ratio could be extracted in the present analysis. Future studies would be centred on modal analysis of the flow fieldto investigate this aspect of the flow behavior and determine to which degree the ground effect interfers with von Karman shedding.

References

[1] Alam, M M, Zhou Y (2007) Phase lag between vortex shedding from two tandem bluff bodies. *Journal of Fluids and Structures*, vol. 23, pp. 339–347.

[2] Astarita T (2006) Analysis of interpolation schemes for image deformation methods in PIV: effect of noise on the accuracy and spatial resolution. *Experiments in Fluids*, vol. 40, pp. 977-987.

[3] Astarita T (2007) Analysis of weighting windows for image deformation methods in PIV. *Experiments in Fluids*, vol. 43, pp. 859-872.

[4] Astarita T, Cardone G (2005) Analysis of interpolation schemes for image deformation methods in PIV. *Experiments in Fluids*, vol. 38, pp. 233-243.

[5] Bhattacharyya S, Dhinakaran S (2008) Vortex shedding in shear flow past tandem square cylinders in the vicinity of a plane wall. *Journal of Fluids and Structures*, vol. 24, pp. 400–417.

[6] Fey U, König M, Eckelmann H (1998) A new Strouhal–Reynolds-number relationship for the circular cylinder in the range $47 < Re < 2 \times 10^5$. *Physics of Fluids*, vol. 10, pp. 1547-1549

[7] Harichandan A B, Roy A (2012) Numerical investigation of flow past single and tandem cylindrical bodies in the vicinity of a plane wall. *Journal of Fluids and Structures*, vol. 33, pp. 19–43.

[8] Igarashi T (1981) Characteristics of the flow around two circular cylinders arranged in tandem (1st report). *Bulletin of the JSME*, vol. 24, pp. 323-331.

[9] Lei C, Cheng L, Kavanagh K (1999) Re-examination of the effect of a plane boundary on force and vortex shedding of a circular cylinder. *Journal of Wind Engineering & Industrial Aerodynamics*, vol. 80, pp. 263–286

[10] Mahir N (2009) Three-dimensional flow around a square cylinder near a wall. *Ocean Engineering*, vol. 36, pp. 357–367.

[11] Martinuzzi R J, Bailey S C C, Kopp G A (2003) Influence of wall proximity on vortex shedding from a square cylinder. *Experiments in Fluids*, vol. 34, pp. 585–596.

[12] Price S J, Sumner D, Smith J G, Leong K, Païdoussis M P (2002) Flow visualization around a circular cylinder near to a plane wall. *Journal of Fluids and Structures*, vol. 16, pp. 175–191.

[13] Shi L L, Liu Y Z, Wan J J (2010) Influence of wall proximity on characteristics of wake behind a square cylinder: PIV measurements and POD analysis. *Experimental Thermal and Fluid Science*, vol.

34, pp. 28–36.

[14] Sumner D (2010) Two circular cylinders in cross-flow: A review. *Journal of Fluids and Structures*, vol. 26, pp. 849-899.

[15] Wang X K, Hao Z, Tan S K (2013) Vortex-induced vibrations of a neutrally buoyant cylinder near a plane wall. *Journal of Fluids and Structures*, vol. 39, pp. 188–204.

[16] Wang X K, Hao Z, Zhang J-X, Tan S K (2014) Flow around two tandem square cylinders near a plane wall. *Experiments in Fluids*, vol. 55, art. 1818

[17] Wang X K, Tan S K (2008) Comparison of flow patterns in the near wake of a circular cylinder and a square cylinder placed near a plane wall. *Ocean Engineering*, vol. 35, pp. 458–472.

[18] Westerweel J, Scarano F (2005) Universal outlier detection for PIV data. *Experiments in Fluids*, vol. 39, art. 1096100

[19] Xu G, Zhou Y (2004) Strouhal numbers in the wake of two inline cylinders. *Experiments in Fluids*, vol. 37, pp. 248–256.

[20] Zdravkovich M M (1987) The effect of interference between circular cylinders in cross-flow. *Journal of Fluids and Structures*, vol. 1, pp. 239-261.

[21] Zhou Y, Yiu M W (2006) Flow structure, momentum and heat transport in a two-tandem-cylinder wake. *Journal of Fluid Mechanics*, vol. 548, pp. 17-48.

[22] Zovatto L, Pedrizzetti G (2001) Flow about a circular cylinder between parallel walls. *Journal of Fluid Mechanics*, vol. 440, pp. 1-25.